

## LETTER TO THE EDITOR

### NMR measurements on intercalated $3R\text{-TaS}_2 \cdot I_x$ ( $I = \text{NH}_3$ and $\text{N}_2\text{H}_4$ )<sup>†</sup>

N H Handly<sup>‡</sup> and J V Acrivos<sup>§</sup>

<sup>‡</sup> California Institute of Technology, Pasadena, CA91125, USA

<sup>§</sup> Trinity College, Cambridge, CB2 1TQ, UK

Received 22 December 1983

**Abstract.** Proton nuclear magnetic resonance was used to probe the environment of the intercalant molecule in low dimensional (aeolotropic) solids  $3R_1\text{-TaS}_2(\text{NH}_3)_{2/3}$  and  $3R_{11}\text{-TaS}_2(\text{N}_2\text{H}_4)_{4/3}$ , and, specifically to look for phase transitions associated with changes in superlattice geometry. The proton resonance frequency for the intercalated molecules in the temperature interval 200 to 300 K indicates that there are different magnetic environments in three temperature domains. (i) There is only one resonance field for molecules in isotropic magnetic environments. (ii) The high- and low-temperature domains (I and III) have molecules in only two different environments, whereas in the middle temperature domain (II) there are at least four different magnetic environments. (iii) The different magnetic environments measured by the ratio of anisotropic to isotropic resonance absorption intensity ( $r_{ai}$ ) indicate that the ratios  $r_{ai}$  are constants of the sample in domains I and II. (iv) At low temperatures (domain III),  $r_{ai}$  depends on magnetic field polarisation effects and the temperature treatment of the sample. We conclude that the different magnetic environments observed for ammonia and hydrazine appear to be determined by the host, octahedrally coordinated  $\text{TaS}_2$ .

The phase transitions that are caused by the intercalation of low dimensional solids (LDS) have important applications leading to new solid catalysts, conductors and battery materials. For this reason there has been recently a concentrated effort directed to determining the parameters which govern reaction (1):

$$L(\varphi_1) + xI(g) - LI_x(\varphi_2) \quad (1)$$

where  $\varphi_1$  is the pristine initial crystal phase and  $\varphi_2$  is the intercalated phase. This is a complex process which involves at least three steps. First Langmuir absorption of the adduct gas must occur; it is followed by chemisorption and finally insertion of the adduct in between the layers produces a phase transition. The understanding of reaction (1) was strengthened by spectroscopic (Beal and Acrivos 1978) and structural measurements by transmission electron microscopy (TEM) of  $\text{N}_2\text{H}_4$  *in situ* intercalated  $\text{TaS}_2$  polymorphs. These indicate (Tatlock and Acrivos 1978) that the in-plane translational symmetry is reduced by intercalation in a precise way which depends on the solid and on the temperature and pressure. The periodic lattice distortion (PLD) describes the dichalcogenide by an empirical formula  $\text{T}_y\text{X}_{2y}$  with  $y \geq 3$ , where  $10^3$  formula units are held

<sup>†</sup> This work is dedicated to Professor R W Vaughan of Cal. Tech., whose untimely death (1978) left a void that has not to this day been filled. The NMR work was done in his laboratory.

<sup>§</sup> To whom all correspondence is to be addressed. Permanent address: San José State University, San José, CA 95192, USA.

together by layers of adduct I. The value of  $y$  is accurately determined from the PLD wavevectors which describe the Bloch functions of the partially occupied orbitally degenerate states of the metal or semimetal and give rise to the distortion according to the Jahn–Teller theorem (Hughes 1977, Acrivos 1974). The existence of localised electron states indicated by the PLD have led to transport and infrared spectroscopic measurements (Sarma *et al* 1982) which allow an estimate of a semiconductor energy gap of the order of half an electron volt in phase  $\varphi_2$ . The existence of localised paramagnetic states was verified by ESR absorption measurements near 4.2 K (Guy *et al* 1982). Nuclear magnetic resonance spectroscopy (NMR) and neutron diffraction offer another means for studying these intercalated solids. Both techniques have been used to probe the intercalant molecule and its macro-environment within the crystal, so far yielding information about the mobility of ammonia and the geometries of ammonia and pyridine in 2H-TaS<sub>2</sub> (Gamble and Silbernagel 1975, Bray and Sauer 1972). The NMR evidence suggests that the ammonia molecule is sensitive to phase changes associated with superlattice formation in intercalated 2H-TaS<sub>2</sub>. The ability to study phase behaviour in intercalated 1T-TaS<sub>2</sub> at a microscopic level would greatly add to our understanding of these materials. This work reports NMR studies of 3R<sub>I</sub>-TaS<sub>2</sub>(NH<sub>3</sub>)<sub>2/3</sub> and 3R<sub>II</sub>-TaS<sub>2</sub>(N<sub>2</sub>H<sub>4</sub>)<sub>4/3</sub> between 200–300 K (Acrivos 1979, Acrivos *et al* 1981).

The crystals of 1T-TaS<sub>2</sub> used in this work were grown by Meyer *et al* (1975) and A Beal and S N Nulsen (Sarma *et al* 1982). The NMR samples were prepared by placing a single crystal in a flattened tube to facilitate rotational studies which was then connected to a vacuum line for intercalation. Ammonia and hydrazine were purified prior to exposure to the crystals. Ammonia was condensed on sodium to remove traces of water and then the gas was admitted to the sample. Freeze-dried hydrazine was distilled *in situ* and then admitted to the sample. The ammonia pressure was 700 Torr and the hydrazine vapour pressure was 12 Torr. After one week at room temperature, the sample tube was immersed in liquid nitrogen and the tube sealed by melting the glass.

The spectra were collected at 56.4 and 13.1 MHz. Free induction decays were collected for time averaging and were then Fourier transformed to give the absorption spectra. Temperature in the probe was varied and regulated to within  $\pm 0.5^\circ\text{C}$  of the desired value by heating nitrogen gas. Resonance frequency assignments were facilitated with the use of an acetyl chloride reference with an accuracy of  $\pm 10$  Hz.

Over the 200–300 K range studied there were three kinds of spectra for 3R<sub>I</sub>-TaS<sub>2</sub>(NH<sub>3</sub>)<sub>2/3</sub> which define three temperature domains. Evidence of the three domains were also found in the spectra of 3R<sub>II</sub>-TaS<sub>2</sub>(N<sub>2</sub>H<sub>4</sub>)<sub>4/3</sub> which were qualitatively the same as the spectra of ammonia intercalated 1T-TaS<sub>2</sub>.

Two resonance lines were found in domain I (250–300 K). The resonance position of one was insensitive to crystal orientation in the magnetic field while the position of the other line was determined by the angle between the crystal  $c$  axis and static magnetic field vector  $H$ . The separation in frequency of the anisotropic and isotropic signals could be approximated by the relation

$$\nu_a - \nu_i = 1.5 A \cos^2 \theta$$

where  $\nu_a$  and  $\nu_i$  are line positions in Hz,  $1.5 A$  is the maximum separation in Hz and  $\theta$  is the angle between the crystal  $c$  axis and  $H$ . Shown in figure 1 are plots of  $(\nu_a - \nu_i)$  versus  $\theta$  for ammonia and hydrazine intercalated samples. These follow the  $(3 \cos^2 \theta - 1)/2$  law for a Knight shift of  $K = A/56.1$  PPM given in table 1.

The ratio of intensities of the anisotropic to isotropic NMR absorption ( $r_{ai}$ ) was also a feature that characterised each temperature domain. In domain I,  $r_{ai}$  was a constant of

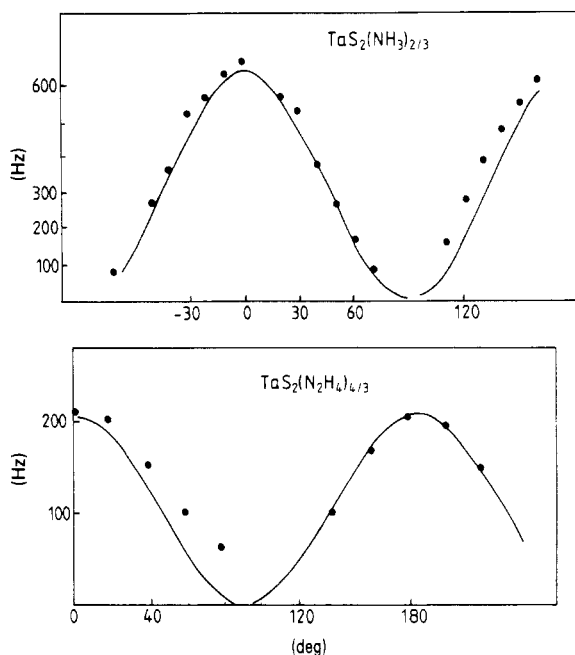


**Figure 1.** Frequency separation between the anisotropic and isotropic proton NMR lines in Hz versus  $\theta$  in degrees for  $3R_I\text{-TaS}_2(\text{NH}_3)_{2/3}$  (sample 1) and  $3R_{II}\text{-TaS}_2(\text{N}_2\text{H}_4)_{4/3}$ . Full circles (●) show collected data with errors in frequency of  $\pm 10$  Hz and in angle of  $\pm 3^\circ$ . The full curve is the plot of  $1.5 A \cos^2 \theta$ , where  $A$  is given in table 1.

**Table 1.** Values of  $1.5 A$  at 56.4 MHz (maximum separation in Hz of the anisotropic and isotropic lines) for different temperatures.

Sample		$T > 250$ K	Multiple lines					$A_I/A_{III}$
			$250 \text{ K} > T > 245 \text{ K}$					
$\dagger \text{ } 3R_I\text{-TaS}_2\text{-(NH}_3)_{2/3} \pm \delta$	(1)	640	530	300	130	110	260	2.46
	(2)	500	400	220	90	—	360	1.38
$\dagger \text{ } 3R_{II}\text{-TaS}_2\text{-(N}_2\text{H}_4)_{4/3} \pm \delta$	(2)	200	—	—	—	—	55	3.63

† The error  $\delta$  in stoichiometry is less than ten per cent of  $x$ .

the sample and not affected by variation of  $\theta$  or temperature. That  $A$  is proportional to the applied magnetic field was verified by carrying out measurements at  $\nu = 56.4$  and 13.1 MHz. A representative spectrum of  $3R_I\text{-TaS}_2(\text{NH}_3)_{2/3}$  is shown in figure 2(a).

In domain II (245–250 K) spectra of  $3R_I\text{-TaS}_2(\text{NH}_3)_{2/3}$  were characterised by the presence of at least five lines; one isotropic and three or four anisotropic. For each of the anisotropic absorptions, the separation from the isotropic line follows the  $A \cos^2 \theta$  behaviour. A representative spectrum for  $\theta = 0^\circ$  is shown in figure 2(b). When all the lines collapse at  $\theta = 90^\circ$ , the linewidth is equal to that of the isotropic line. As was observed in domain I, the  $r_{ai}$  values for all anisotropic lines were constants of the sample. For  $3R_{II}\text{-TaS}_2(\text{N}_2\text{H}_4)_{4/3}$  there was an isotropic line and an unresolved manifold of several lines that collapsed at  $\theta = 90^\circ$  showing a maximum separation at  $\theta = 0^\circ$ .

In domain III (200–245 K) there were two lines which showed the orientational dependence observed in domain I. However, there was a striking feature in this tem-

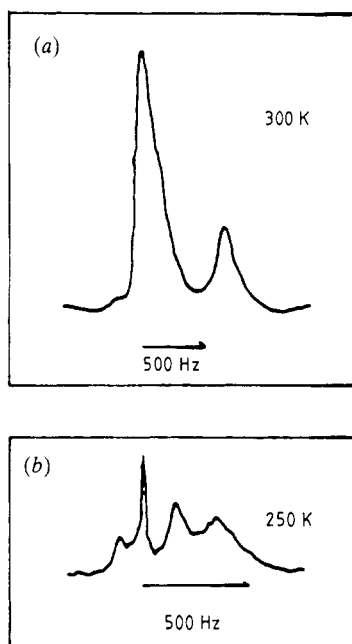


**Figure 2.** NMR absorption representative spectra of  $3R_1\text{-TaS}_2(\text{NH}_3)_{2/3}$  (sample 1). (a) At room temperature and  $\theta = 0^\circ$ . The anisotropic peak is at the right at higher frequency. The arrow is a 500 Hz standard and points to higher frequency. (b) At 250 K and  $\theta = 0^\circ$ .

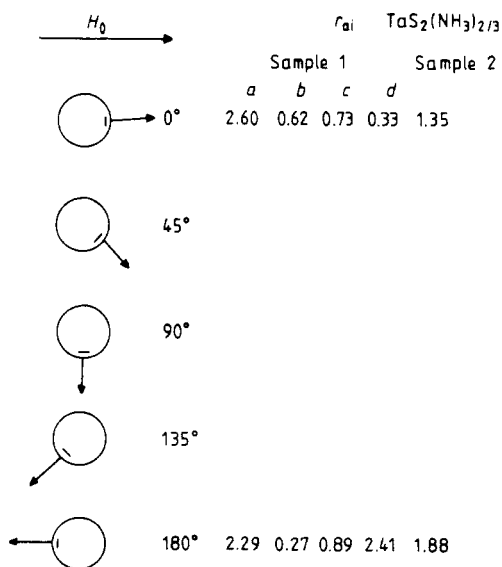


**Figure 3.** Illustration of how rotation of a sample cooled to a temperature below 245 K affects  $r_{ai}$ , the ratio of anisotropic to isotropic line intensity, for five different cooling cycles of sample 1 in table 1. A view down the instrument probe is shown to highlight the importance of the angle between the crystal  $c$  axis and the magnetic field. The crystal is seen edge-on and is pictured in an exaggerated off-axis position to help distinguish angles  $\theta = 0^\circ$  and  $\theta = 180^\circ$ .

perature domain which was not observed in domains I or II. Each time any samples were cooled,  $r_{ai}$  would take on randomly two new values that would reversibly interconvert as the crystal was rotated through  $\theta = 90^\circ$  or  $\theta = 270^\circ$ . Figure 3 illustrates the change in  $r_{ai}$  upon rotation and contains pairs of  $r_{ai}$  values from several coolings.

Our work shows that proton NMR of the guest molecules within  $\text{TX}_2$  is a good probe of the magnetic micro-environments within intercalated complexes. NMR reveals the presence of two micro-environments within the complexes as well as a phase transition at 245–250 K, most likely associated with the change in superlattice geometries observed in that temperature range by other methods. The significant observations are as follows:

(i) Crystals intercalated with  $\text{NH}_3$  and  $\text{N}_2\text{H}_4$  both show the same two-line pattern where the position of the low-frequency peak is independent of, and the high-frequency peak is dependent upon, the orientation of the crystal within the magnetic field. The proton linewidths observed are consistent with a rapid reorientation of  $\text{NH}_3$  and  $\text{N}_2\text{H}_4$  molecules within the layers. This is in agreement with the measurements made by Silbernagel and Gamble on  $2\text{H-TaS}_2(\text{NH}_3)_x$ , but in this metallic complex the Knight shift is one order of magnitude greater than for the  $3\text{R-TaS}_2\text{I}_x$ . The different values of  $A$  reported in table 1 suggest that the proton Knight shift is determined by the number of adduct molecules in the complex which localises the electron states.

(ii) Intercalant adduct molecules do not exchange between the two magnetic environments that are the source of the isotropic and anisotropic peaks as there is no evidence of exchange broadening or averaging. This means that the molecular complexes are stable within times longer than  $t \approx (2\pi A)^{-1}$  or  $10^{-3}$  to  $10^{-4}$  s. We offer the following proposal for the identities of the magnetic environments leading to the two lines. The isotropic signal arises from protons in fractured or poorly ordered domains and the anisotropic resonance is a result of adduct molecules occupying an ordered region where a superlattice exists. Fractures and other crystal defects that would prevent superlattice formation have been observed by a number of investigators (Tatlock and Acrivos 1978), and the intercalation process itself may be responsible for some of these faults. Regardless of the cause of the crystal disorder, intercalant molecules in these disordered volumes would not be affected by fields oriented with the crystal geometry and, hence, give rise to the isotropic signal.

(iii) Evidence for a role of superlattices in forming the anisotropic field is twofold. Wilson *et al* (1975) have measured bulk susceptibility in  $1\text{T-TaS}_2$  and found variation of this parameter coincident with different superlattice geometries. Guy *et al* (1982) have observed similar effects in  $3\text{R-TaS}_2(\text{N}_2\text{H}_4)_x$ . Also we find a complex, multiline spectra with one line isotropic and the remainder anisotropic in the 245–250 K region. This is the same temperature range in which Tatlock and Acrivos (1978) observed a superlattice phase transition. In one of the materials we have studied,  $3\text{R}_{\text{II}}\text{-TaS}_2(\text{N}_2\text{H}_4)_{4/3}$ , our spectra suggest that two or more distinct superlattices may be present within the sample in this temperature range as each superlattice would contribute a different susceptibility field and be revealed as distinct anisotropic lines.

(iv) Below 245 K, a two-line (anisotropic and isotropic) NMR signal like the room temperature spectra is found for  $3\text{R}_{\text{II}}\text{-TaS}_2(\text{N}_2\text{H}_4)_{4/3}$ ; however, a smaller separation between the two lines is observed. This is in agreement with the fact that a different superlattice occurs within these crystals in the 200–245 K range (Tatlock and Acrivos 1978) and that a decrease in carriers reduces the Knight shift. Also, in this temperature range, a new pattern of resonance line intensity is observed. The sum of anisotropic and isotropic line intensities is not altered from that value observed at room temperature, so

the total number of protons in the sample remains constant within experimental uncertainty. Yet two discrete ratios of anisotropic to isotropic line intensities are found, one for each face of the crystal (figure 3), that do not change until the sample is warmed above 245 K. In addition, each cooling event yields a new pair of intensity ratios. The variation in intensities of the two peaks, which is not observed at temperatures above 245 K, presents an interesting problem. To account for this particular situation, we propose a mechanism whereby the formation of the superlattice at low temperature is affected by temperature. Each cooling would appear to lead to varying amounts of this superlattice since crystal defects may be locked in or introduced by the temperature change. The anisotropic line intensity would be influenced by the volume of the crystal where the local magnetic fields cancel. While the temperature effects on relative line intensity are unpredictable, the effects of the magnetic field polarisation are not random. Although we are unable to explain this latter phenomenon, our results suggest that future experiments at higher magnetic fields may be able to shed some understanding on the chiral dependence of the NMR absorption below 245 K for samples cooled in a magnetic field. Transport measurements of samples cooled in a magnetic field may also show this chiral dependence if the above model where local magnetic fields cancel in discommensurate Bloch walls is correct. These were predicted by McMillan (1976) and found recently by TEM (Fung *et al* 1981).

We have shown that proton NMR studies of the intercalant molecule with an octahedrally coordinated TaS<sub>2</sub> host are able to describe the phase transition near 245 K, which has not been observable by techniques based upon measurements of bulk properties. Additionally, our findings suggest that intercalant adduct molecules such as ammonia and hydrazine are sensitive to local magnetic fields caused by superlattices. The physical significance is that the random potential fields in the adduct layer can affect the motion of electrons in the TaS<sub>2</sub> layer.

This work was supported in part by NSF DMR 790011 and NATO Grant 1441. J V Acrivos is grateful for a Visiting Fellowship at Trinity College, Cambridge during 1983 and a Sabbatical leave from SJSU. We also thank Miss J Rowe who did the word processing at Trinity College.

## References

- Acrivos J V 1974 *J. Phys. Chem.* **78** 2399  
— 1979 *Physics and Chemistry of Materials with a Layer Structure* Vol. VI, ed. F Levy (Dordrecht: Reidel), pp 33–98  
Acrivos J V, Parkin S S P, Reynolds J R, Code J and Marseglia E 1981 *J. Phys. C: Solid State Phys.* **14** L349–L357  
Beal A R and Acrivos J V 1978 *Phil. Mag.* **37** 409  
Bray D and Sauer E 1972 *Solid State Commun.* **11** 1239  
Fung L, McKernan S, Steeds J W and Wilson J A 1981 *J. Phys. C: Solid State Phys.* **14** 5417  
Gamble F and Silbernagel B 1975 *J. Chem. Phys.* **63** 2544  
Guy D P, Friend R H, Harrison M R, Johnson D C and Sienko M J 1982 *J. Phys. C: Solid State Phys.* **15** L1245  
Hughes H P 1977 *J. Phys. C: Solid State Phys.* **10** L319  
McMillan E L 1976 *Phys. Rev. B* **14** 1496  
Meyer S R, Howard R, Stewart G, Acrivos J V and Geballe T H 1975 *J. Chem. Phys.* **62** 4411  
Sarma M, Beal A, Nulsen S and Friend R 1982 *J. Phys. C: Solid State Phys.* **15** 477  
Tatlock G J and Acrivos J V 1978 *Phil. Mag.* **38** 81  
Wilson J, Di Salvo F and Mahajan S 1975 *Adv. Phys.* **24** 117